DETERMINATION OF THE VELOCITY PROFILES IN RECTANGULAR CHANNELS USING A DOUBLY REFRACTING LIQUID

A THESIS

Submitted to
The Department of Chemical Engineering
of
The University of Tennessee
in
Partial Fulfillment of the Requirements
for the degree of
Bachelor of Science

---

by

Albert Phil Farrow, Jr.

August 1956

ACKNOWLEDGEMENT

The writer wishes to thank Mr. John W. Prados for his direction and supervision of this thesis. Without his enthusiasm and leadership this work would have been impossible. Appreciation is also extended to Mr. H. B. Thompson of the chemical engineering shop staff for his fine work in building the flow channels.

CRANES CREST

TABLE OF CONTENTS

CHAPTER		PAGE
I.	SUMMARY	1
II.	INTRODUCTION	4
III.	THEORETICAL DISCUSSION	6
IV.	MATERIALS AND EQUIPMENT	11
V.	EXPERIMENTAL PROCEDURE	17
VI.	METHODS OF DATA ANALYSIS	20
VII.	RESULTS AND DISCUSSION	32
VIII.	CONCLUSIONS AND RECOMMENDATIONS	38
LIST OF REFERENCES		39
APPENDIX		41

LIST OF TABLES

TABLE		PAGE
I.	Summary of Flow Rate Determinations	33
II.	Calculation of Data for Plotting the Velocity Gradient Curve in a Rectangular Channel . . .	44
III.	Calculation of Data for Plotting the Velocity Profile Curve in a Rectangular Channel . . .	47
IV.	Calculation of Data for Plotting the Velocity Gradient Curve in a Square Channel	52
V.	Calculation of Data for Plotting the Velocity Profile Curve for a Square Channel	54
VI.	Experimental Data	57
VII.	Experimental Data	58
VIII.	Experimental Data	59
IX.	Experimental Data	60
X.	Experimental Data	61
XI.	Experimental Data	62

LIST OF FIGURES

FIGURE		PAGE
1.	A typical arrangement of bands seen in a square or rectangular channel	7
2.	Schematic representation of plane polarized light passing through a doubly refracting liquid	9
3.	Photograph of the experimental equipment	12
4.	Schematic diagram of flow apparatus	13
5.	Schematic diagram of the optical system - top view	14
6.	Typical velocity gradient across channel	23
7.	Typical velocity profile across channel	23
8.	Top views of velocity profiles in square channels	30
9.	Calibration curves of Solution T-2	42
10.	Calibration curves of Solution T-3	42
11.	Rotameter calibration curve	43
12.	Velocity gradient across rectangular channel . .	46
13.	Velocity profile across rectangular channel . .	49
14.	Velocity gradient across square channel	53
15.	Velocity profile across square channel	55

CHAPTER I

SUMMARY

When plane polarized light is passed through a moving, doubly refracting liquid, visible patterns related to the stresses in the fluid may be seen. Aqueous solutions of a commercial dye known as milling yellow possess doubly refracting properties and can be used to analyze stresses in the moving fluid. It was the purpose of this work to obtain the velocity profiles of a milling yellow dye solution pumped through a rectangular Plexiglas channel by visual analysis of the stress patterns.

In passing monochromatic, polarized light through such a dye solution flowing through a transparent channel under laminar conditions, dark parallel bands were observed in the channel. The number and position of these bands varied with the concentration of the dye solution, the temperature, and the flow rate. A sample of the dye solution was analyzed in an instrument known as a concentric cylinder polariscope where the velocity gradient corresponding to each band could be determined. By correlation of this calibration data with the bands observed in the channel and analysis of the results by integration, the velocity profile across the channel could be determined. As a check on the validity of the results, the theoretical flow rate of the solution was obtained by

integration of the velocity curve. The analytically determined flow rate could then be checked against the actual flow rate which was measured by a calibrated rotameter.

All calculated flow rates were checked against the actual flow rates; and for those made for flow in a square channel, the calculated flow rates were very significantly in error. In fact, all the calculated flow rates were far lower than those actually measured. Calculated flow rates for a square channel ranged from 16 per cent too low for a 9 cc. per second measured rate to 52 per cent too low for a flow rate of 107 cc. per second. However, calculations were more valid for flow rates through a rectangular channel. Where a channel with a horizontal width approximately three times that of the vertical width was used, the calculated flow rate was 5 per cent too high for a flow rate of 9 cc. per second when the data were taken without the use of quarter-wave plates. For this same channel, a calculation was made that was in error by only $\pm$ 1 per cent of the measured flow rate of 9 cc. per second when the data were taken with the use of quarter-wave plates.

In conclusion, it may be said that at present there is no known optical method for studying three dimensional flow, but it appears that it is possible to analyze optically two dimensional flow systems which are more nearly produced by rectangular than by square channels. More work

will have to be done with rectangular channels to prove definitely the validity of the present method of analysis.

CRANES CREST

CHAPTER II

INTRODUCTION

In 1953 at the University of Tennessee, studies were begun on the optical and physical properties of solutions of a commercial dye. This dye, known as milling yellow, exhibits doubly refracting properties, i.e., when polarized light is passed through an aqueous solution of this dye set in motion, stress patterns in the fluid can be seen. Since that date, a great deal of work has been done at the University on the properties of this dye - much of this work has been done under the sponsorship of the Office of Naval Research, Contract Nonr-811(04). Investigations have been made on the methods of preparing doubly refracting, aqueous solutions of milling yellow, the viscosity and density of such solutions, and the extent of double refraction as a function of the velocity gradient.

It is often desirable to know fluid behavior as it flows through various channels, through restrictions, and in narrow boundary layers. At present, there is little mathematical knowledge on the analysis of flow situations, most analyses being carried out by quantitatively measuring the flow with probes, etc. Of course, when it is necessary to insert a flow measuring instrument into a system, the flow patterns are often disturbed very noticeably. In these

cases, it would be very desirable to be able to analyze flow situations by visual observation alone. This method becomes possible when plane polarized light is passed through a moving, doubly refracting liquid.

It is the scope of this work to try to establish a definite method of flow analysis by visual observation of milling yellow dye solutions under polarized light. The simplest type of situation was chosen for the study, i.e., unidirectional, laminar flow through a rectangular, plastic channel. A square or rectangularly shaped channel was chosen instead of a circular one, because this permitted observation through a constant thickness of liquid from the top to the bottom of the channel. The object of the flow analysis was to obtain the velocity distribution across the channel without inserting measuring devices into the channel. The flow rate through the channel could then be calculated by integration of the velocity profile, and this could be checked against the actual flow rate as measured by a rotameter.

CRANES CREST

CHAPTER III

THEORETICAL DISCUSSION

When polarized light is passed through a solution of milling yellow dye at rest, no unusual effects are observed. However, when the solution is set in motion, stress patterns are produced in the fluid which show up as dark areas under the polarized light. When white light is used, various colored bands are produced in the solution; but when a monochromatic light source is used, only dark or black bands may be seen.

As mentioned before, only those stresses produced by laminar flow of the dye in rectangular channels under a sodium light were studied. The number and position of the bands formed in the channel by the passage of polarized light through the liquid depend upon the velocity gradient which exists in the channel. This velocity gradient varies with the shape and size of the channel, the fluid temperature, and age and initial concentration of the dye solution. For a particular set of conditions, the bands might align themselves in the channel in a manner like that shown on the following page in Figure 1.

The behavior of plane polarized light in a doubly refracting liquid may be analyzed as follows. When plane polarized light is passed through such a liquid, the ray is

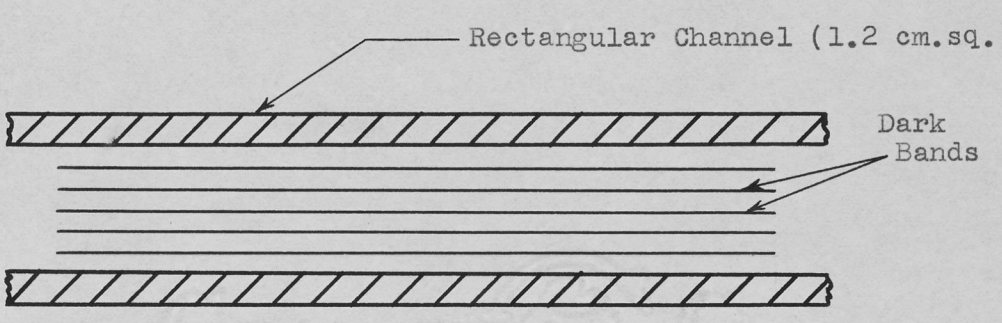


Figure 1. A typical arrangement of bands seen in square or rectangular channels.

broken up into two components, one travelling faster than the other. There exists one direction at any point in the moving liquid known as the optic axis. One component of the ray produced by the double refraction vibrates perpendicular to this optic axis with a velocity independent of its direction of propagation. This component is called the ordinary ray. The other component produced by double refraction is a ray vibrating parallel to the optic axis and travelling in a direction perpendicular to it. This component is called the extraordinary ray.

As these two components have different velocities, one will emerge from the liquid a small time interval after the other (Δt). Since both rays travel in air with the same velocity, the extraordinary ray will be retarded behind the ordinary ray by a certain distance (δ). It has been found that this retardation is a function of the rate of shear present in the moving liquid and the thickness of

liquid through which the rays travel. Therefore, in a moving doubly refracting liquid under given experimental conditions, there is a definite relationship between the number of stress bands observed and the rate of shear of the moving liquid.

To examine the phenomenon of double refraction more closely, it is convenient to analyze a tiny element of moving liquid under constant stress throughout, and illuminated by parallel rays of light passed through crossed polarizing plates (their axes set 90° to each other). Reference to Figure 2, page 9, will show the effects of passing a single polarized light ray through a tiny element of liquid.

Parallel rays of light approaching from the left are allowed to vibrate in only one direction (OX) by the polarizer plate. When entering the moving, doubly refracting liquid, shown at center, the light ray is broken up into two components, the ordinary ray and the extraordinary ray as mentioned before. These two components are represented in Figure 2 by u_1 and u_2, respectively. The two components leave the liquid vibrating in different directions; but when they reach the second polarizer plate, the analyzer, only the resultant of these two components (w) is allowed to pass through.

By equations for the periodic motion of the plane polarized light and certain trigonometric relationships, it

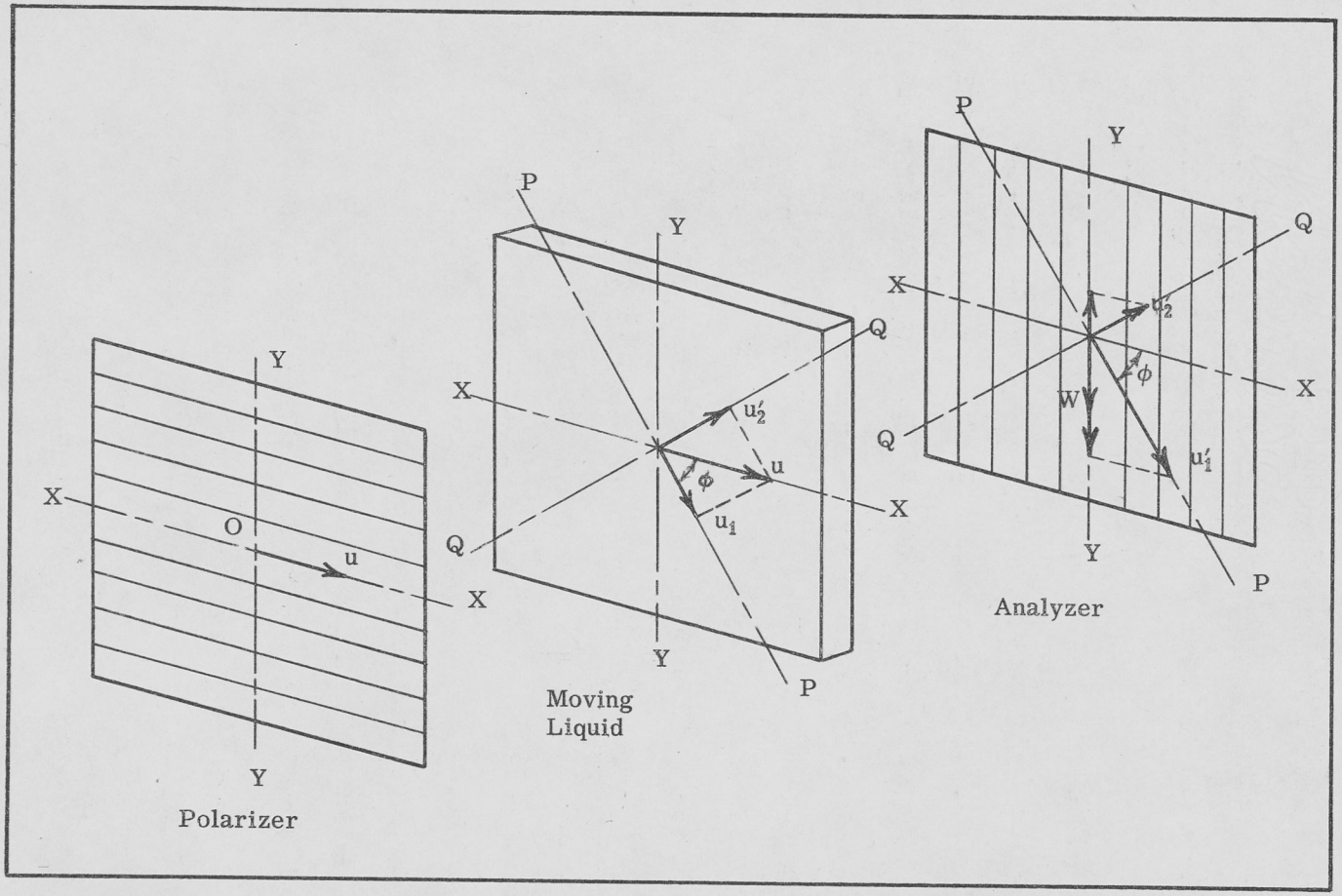


Figure 2. Schematic Representation of Plane Polarized Light Passing Through a Doubly Refracting Liquid.

can be shown that a dark band will appear when the relative retardation between the two light components leaving the liquid (δ) is a distance equal to an integral number of wave lengths of the light employed. Represented mathematically, this is,

$$\delta = N\lambda$$

where

δ = distance of retardation

λ = wave length of light used

N = 0, 1, 2, 3, 4, . . .

Thus, a dark band will be observed when the retardation is one wave length (N = 1), when the retardation is two wave lengths (N = 2), etc.

A more detailed explanation of the mathematics involved in double refraction is given by Peebles (3).

CRANES CREST

CHAPTER IV

MATERIALS AND EQUIPMENT

The experimental equipment used in the study of flow visualization had been set up previously by John W. Prados. The only additions made were the building of two different types of flow channels.

The fluid in the system under study was a solution of about 1.3 per cent by weight of milling yellow dye dissolved in water. As temperature variations cause marked changes in the flow patterns, it was necessary to keep the apparatus in an air conditioned room. A temperature of about 24.5°C. was maintained in the room, and this proved quite satisfactory for the work. The temperature of the solution was controlled by a constant temperature bath set between 23-24°C. Most visualization patterns were measured at a channel temperature between 24.5-25.0°C., and it was necessary to keep the bath at a lower temperature due to the heating effect of the circulating fluid.

A photograph of the general experimental system is shown in Figure 3. Figures 4 and 5 are schematic drawings of the flow and optical systems, respectively.

Reference to Figure 4 will give a rough idea of the flow set up. The dye solution flowed from the constant temperature bath to a centrifugal pump driven by a 1.5 h.p.

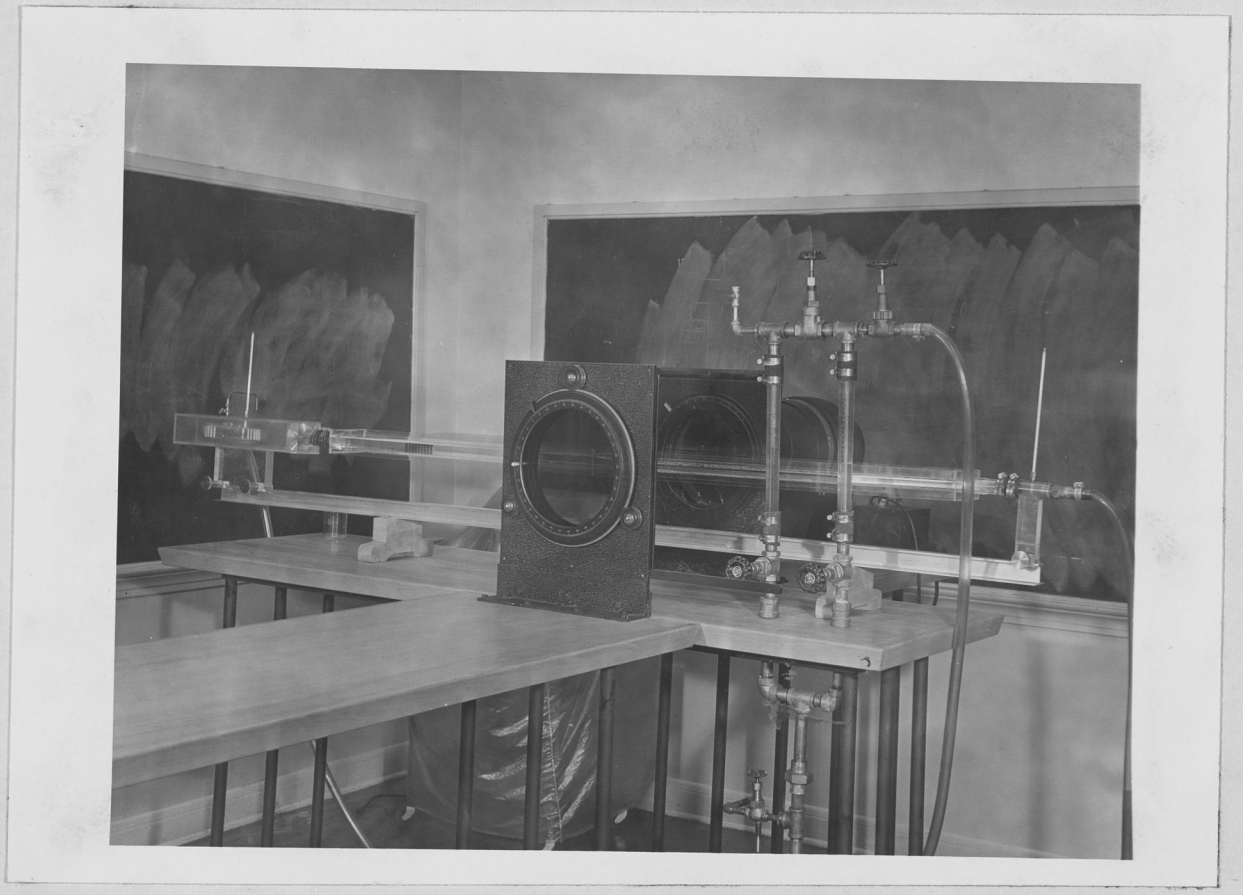


Figure 3. Photograph of the Experimental Equipment.

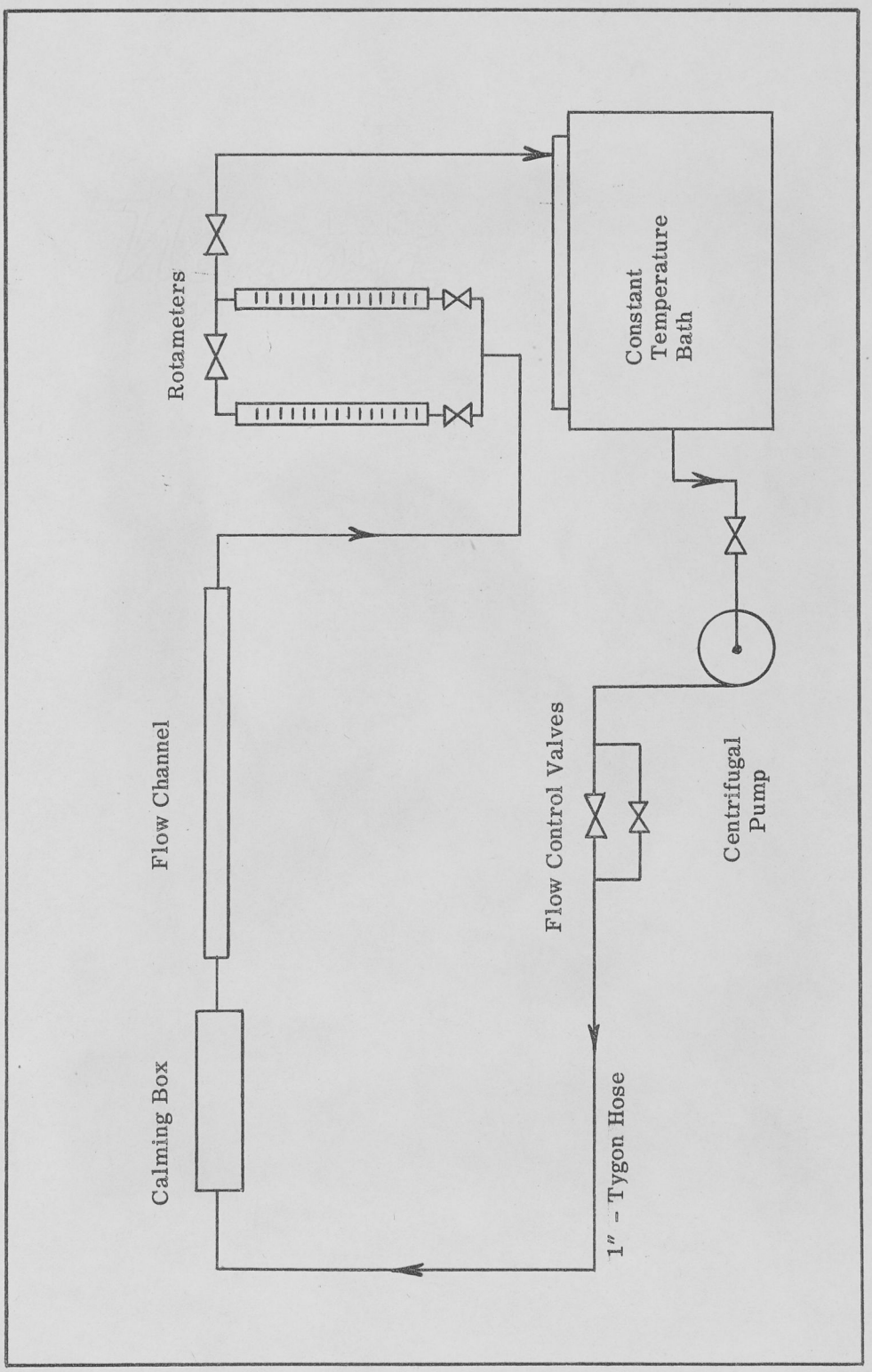


Figure 4. Schematic Diagram of Flow Apparatus.

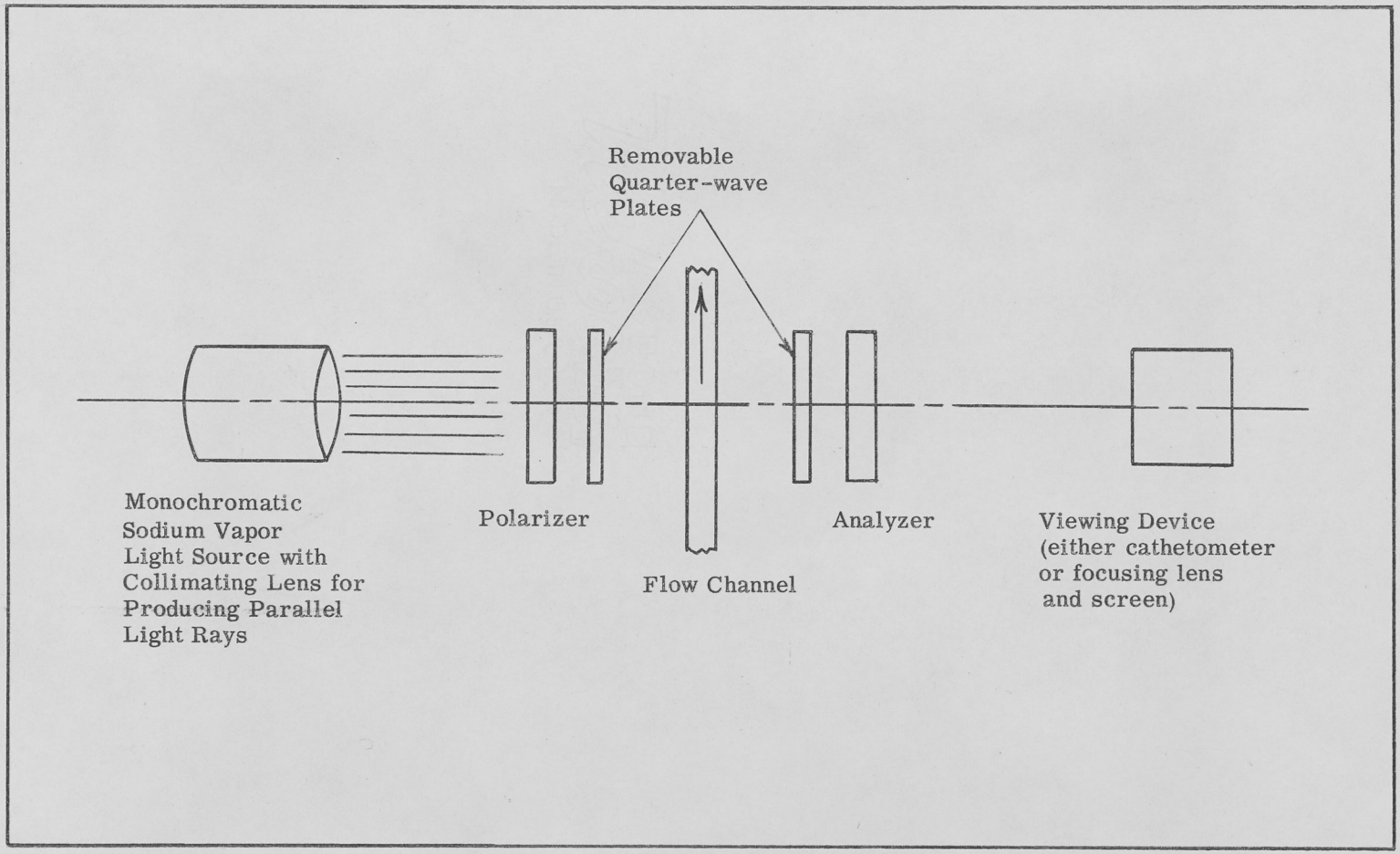


Figure 5. Schematic Diagram of the Optical System - Top View.

electric motor. At the pump outlet two valves were used for flow rate control, a gate valve for large flow rate changes and a needle valve for finer adjustments. From the pump the fluid travelled through Tygon hose to a small reservoir or calming box and into the particular channel under study. As indicated in Figure 4, the fluid flowed from the channel to a rotameter through a connecting Tygon hose and thence back into the constant temperature bath. This same pump and temperature bath also served another flow visualization set up not used in this experiment.

In Figure 5 is given a schematic diagram of the optical system used in the experimental work. A sodium vapor lamp was used for the light source. On each side of the flow channel were mounted the circular polarizer and analyzer plates, each 10 inches in diameter. The plates were fastened so that they could be rotated to any desired angle. Mounted adjacent to each of the polaroid plates were quarter-wave plates of the same diameter. These quarter-wave plates were fastened on slides so that they could be pulled from in front of the polaroid plates if desired.

As illustrated in Figure 5, the spacing of the dark bands formed in the channel was measured with a cathetometer. The cathetometer was equipped with a cross-hair telescope and was placed several feet from the analyzer plate and in line with the sodium lamp and polarizer plate. The telescope

could be moved up or down either electrically or by hand. The height of the telescope relative to an arbitrary zero position was recorded on a dial. This cathetometer could be read to 0.01 mm., which is more precision than this work justifies.

Velocity profiles in three types of flow channels were studied. The first experimentation was done using a square flow channel. The channel was constructed of Plexiglas and measured 1.2 x 1.2 cm. I.D. by 90 cm. long. The channel was constructed with cylindrically shaped end pieces so that it could be quickly and easily coupled into the flow system. The pieces were carefully glued together so that the inner surfaces would be smooth and free from any obstructions that might disturb the flow pattern.

The second type of channel studied was a modified form of the first. This channel was built identical to the first except that four thin metal strips (of shim stock) were mounted parallel to each other in one end of the channel. The strips extended about 1 foot from the end into the channel.

The third channel was constructed of Plexiglas in a manner similar to that of the first channel described. This channel was 90 cm. long with its interior dimensions measuring 1.3 x 3.8 cm. This channel was installed in the flow set up with its longest inside dimension horizontal.

CHAPTER V

EXPERIMENTAL PROCEDURE

The experimental procedure for gathering data was relatively simple. Before any measurements could be made, it was necessary to allow the sodium lamp to warm up for about 15 minutes until it reached full intensity. The dye solution was circulated through the flow system by the centrifugal pump (see Figure 4, page 13), and the flow rate was adjusted with the gate and needle valves. The fluid was circulated until its temperature rose to approximately 24.5°C. (measured just down stream from the test section), at which temperature it was desired to record all experimental data. By setting the constant temperature bath at about 23.5°C., the temperature would rise in 10-15 minutes to approximately 24.5°C. where it would remain practically constant for some time. After the fluid had been circulated a good while, it was necessary to turn off the pump and allow the temperature bath to cool the liquid.

Once a temperature of about 24.5°C. was reached, the flow was adjusted to the desired rotameter setting. For flow rates lower than those giving a rotameter setting of 170 (107 cc. per second), it was necessary to have a second person continually adjust the needle valve in order to maintain a constant flow. Above a rotameter setting of 170, the flow

rate remained constant, without adjustment, to within plus or minus one division on the rotameter scale (±0.63 cc. per second).

Upon obtaining the desired channel temperature and flow rate, the position of each band in the channel was measured with the cathetometer. In using the cathetometer, it was found convenient to traverse the vertical tube distance once from top to bottom measuring each band and adjusting the instrument by hand. The cathetometer reading was recorded for the inside top of the channel, each successive band, and finally for the inside channel bottom. The horizontal width of the channel was also measured with the cathetometer by rotating the channel a half-turn about its long axis.

A second method of measuring the band positions in the tube was tried. This method consisted of projecting the flow pattern onto the wall with a large condenser lens. The lens was placed about 1 yard directly in front of the analyzer plate, and the image was projected onto a clip board fastened to the wall about 8 feet away. It was necessary to make these measurements at night as the room had to be in complete darkness for the image to be seen. A sheet of paper was fastened to the clip board, and marks were made on the paper corresponding to the tube walls and position of the bands in the tube. This method, however, proved to be more

troublesome and less accurate than the cathetometer measurements. The main advantage of the method was that readings could be quickly taken before the temperature of the solution changed.

Several rotameter calibrations were made in order to obtain the volumetric flow rate for each particular setting. The most convenient method of calibration was one of continuous weighing. The solution at a particular flow rate was directed into a large container sitting on a balance. When the scale balanced a stop watch was started and a weight put on the scale. After the scale balanced again, the time interval and weight of fluid collected were recorded. A density measurement was run on the fluid using a Whestphal balance. The density of the solution used was found to be 1.002 gm. per cc. at 25°C.

CHAPTER VI

METHODS OF DATA ANALYSIS

As was stated in Chapter III, the dark bands observed in the channel are a function of the shearing stress in the liquid; and each band should represent a definite rate of shear or rate of change of velocity. Thus, if it were possible to assign a definite rate of shear to each respective band occurring for a particular flow rate, one would be able by integrations to obtain the velocity profile and flow rate through the channel.

From the previous work of Prados (5) and others, a method was available whereby the definite rate of shear of each band could be determined. This method involved the use of a device known as a concentric cylinder polariscope. The work of obtaining band calibration with this instrument was not within the scope of this thesis, and these data were obtained by Prados (4). A detailed explanation of the principles and operation of the concentric cylinder polariscope is given by Prados (5).

The general principle behind operation of the concentric cylinder polariscope is as follows. A sample of the milling yellow dye solution to be calibrated is placed in the instrument between two concentric cylinders. The inner cylinder is stationary and the outer, with glass top and

bottom windows, is connected by belt and pulley to a variable speed drive motor. A known velocity gradient is set up in the liquid as determined by the speed of the rotating outer cylinder and radial distance between the two cylinders. A monochromatic light source is used to pass polarized light vertically up through the fluid in the annulus.

As the speed of the outer cylinder of the concentric cylinder polariscope is increased, dark circles appear in the annulus. The first circle corresponds to the first order fringe where N = 1 (refer to equation on page 10), and the retardation distance (δ) is equal to one wave length (λ) of the light used. The second circle in the annulus appears when the retardation distance is equal to two wave lengths of the light used or when N = 2, and so on for the succeeding circles. By this method of analysis, with certain corrections applied, it was possible to obtain a curve of band order versus rate of shear in $sec.^{-1}$ for a given solution. Examples of such calibration curves are given in Figures 9 and 10 in the Appendix.

Using the data from the band calibration curves and the data giving the band positions in the channel as measured by the cathetometer, calculations were made to determine the velocity profiles and flow rates through the channel. The initial step in making these calculations was to plot the rate of shear ($sec.^{-1}$) of each respective band observed in

the channel versus the distance of that band from the channel wall. The first group of these integrations was made by assigning the center band observed in the channel a zero rate of shear. The bands on each side of the center band were assigned rates of shear corresponding to those of bands 1, 2, 3, etc. on the calibration curve. Upon making these plots, curves similar to the one shown in Figure 6, page 23, were obtained.

The next step toward obtaining the velocity profile across the channel was to calculate the areas under the velocity gradient curves by graphical integration. The approximate integration was carried out in the following manner. The abcissa of the velocity gradient curve was divided into a number of intervals like those numbered 1 to 3 in Figure 6. The area under the curve within each interval was obtained, and the successive areas were added to each other to obtain the velocity at that particular point in the channel. A velocity of zero was assigned to the fluid at the walls. When a plot of these velocities versus the distance across the channel was made, a velocity profile curve similar to that shown in Figure 7, page 23, was obtained. Due to experimental errors, the area under the left half of the velocity gradient curve was not always exactly equal to the area under the right half. For this reason, the points do not coincide at the center of the plot as illustrated in

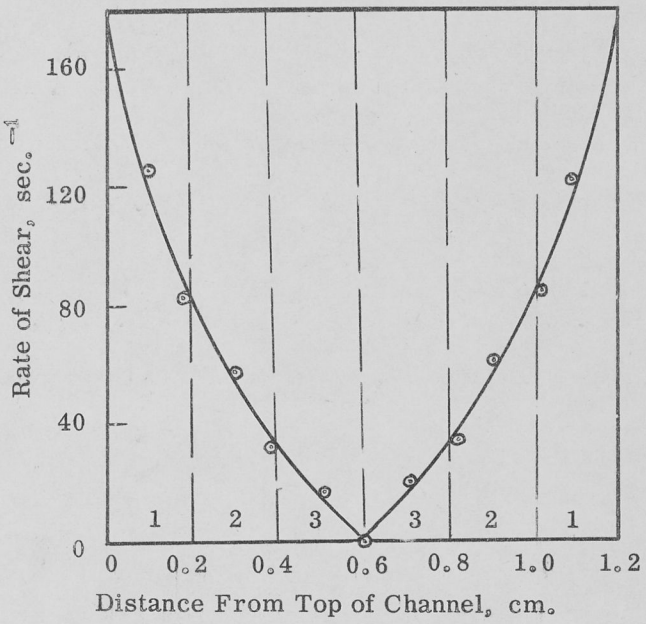


Figure 6. Typical Velocity Gradient Across Channel.

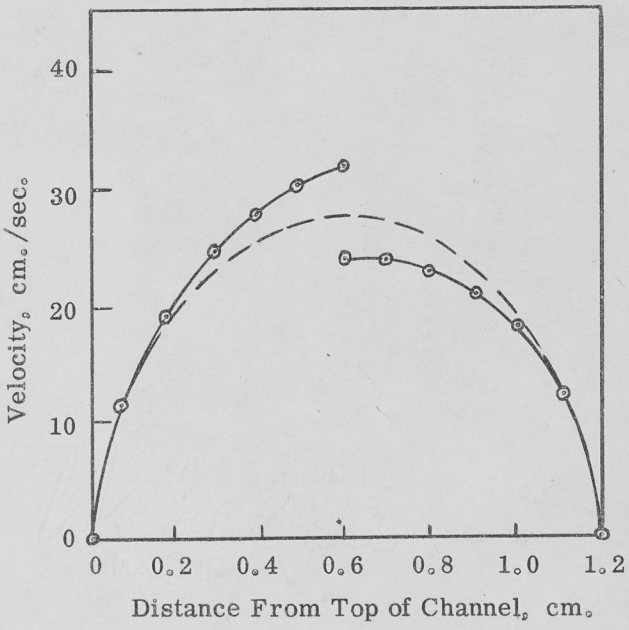


Figure 7. Typical Velocity Profile Across Channel.

Figure 7, and the velocity profile is drawn through the mean of the points.

These velocity profile curves obtained by integration of the velocity gradient curves represent the average velocity across the horizontal width of the tube. They should not be confused with a velocity profile through the center of the tube. As the velocity at any point on the curve is the average velocity across the entire channel, the area under this curve (sq. cm. per second) when multiplied by the thickness of the channel (cm.) should give the volumetric flow rate through the channel (cu. cm. per second). However, the volumetric flow rates obtained by these integrations did not agree at all with the flow rates measured by the rotameter. In fact, the calculated flow rates were all much lower than the actual flow rates, and the percentage error in the calculated flow rates ranged from 50 to 90 per cent over the range studied.

In attempting to discover the reason for these large discrepancies, the formation of bands in the channel with increasing flow rates was studied. These studies were made, like the analysis above, using quarter-wave plates. When the dye solution was motionless, the channel appeared dark, and no bands were observed. As the control valve was opened a slight amount and the fluid set in motion, a band appeared in the center of the channel. As the flow rate was continually

increased, bands emerged simultaneously from the top and bottom walls of the channel and crowded toward the center band. Moreover, it was observed that these bands would merge with the center band. Perhaps there would be seven bands in the channel; and as the flow rate was increased slightly, the two bands on each side of the center band would merge with the center band. Other mergers of the bands adjacent to the center band were observed at increased flow rates. Of course, while the flow rate was increased, additional bands would move out from the top and bottom walls irrespective of the band mergers occurring at the center of the channel.

The previously described analyses were carried out using quarter-wave plates. In the experimental set up, the quarter-wave plates were mounted adjacent to the analyzer and polarizer plates (refer to Figure 5, page 14). The function of these plates was to convert the plane polarized light, vibrating in one direction only, to circularly polarized light. Theoretically, the same pattern of stress bands should be observed in the channel whether or not the light is plane or circularly polarized. A more detailed explanation of this theory can be found in Frocht (1).

Another study was made of the formation of bands in the channel with increasing flow rates, but this time the study was made without the use of quarter-wave plates. It

was found, contrary to expectation, that the removal of the quarter-wave plates altered the pattern of bands seen in the channel. Approximately the same number of bands appeared under the plane polarized light, but the distance between the center band and the two bands adjacent to it was generally greater than was observed under the circularly polarized light. However, the most significant difference was in the merger of the bands. Bands moved out from the walls and merged as they did with the quarter-wave plates in position, but this time the mergers occurred with the bands on each side of the center band. Unlike the mergers observed with the quarter-wave plates, the same band remained in the center of the channel under the plane polarized light.

Various methods of calculation were used to analyze the data obtained from the observations made under both the plane and the circularly polarized light. Studies of stress analysis indicate that systems of shear stresses which are coplanar with the direction of the polarized light rays produce no photoelastic effect. This phenomenon is explained more fully by Frocht (2). The above statement is a very good basis for assigning the center band formed in the channel under any laminar flow conditions a zero rate of shear. This means that the formation of the bands should not be affected by the shearing stress of the channel walls in the line of sight. Another reason why the center band must be

assigned a zero rate of shear is that any finite shearing stress assigned to the center band will result in a sharp-nosed velocity profile upon integration of the velocity gradient curve. Previous experimenters have established the fact that velocity profile curves should be round-nosed.

In spite of the above arguments, it was still difficult to see how bands corresponding to a definite rate of shear could move into the center of the channel and merge with the zero order band. At the first of this chapter a method of integration was described which disregarded the merger of the bands observed with the quarter-wave plates. A second method of calculation was tried in which an empirical correction factor was applied. The center band was corrected from a definite rate of shear given by the number of mergers down to a zero rate of shear. The other bands were corrected a proportional amount in a linear relationship from this maximum correction at the center of the channel to a zero correction at the walls. The corrected rates of shear corresponding to each band were plotted against the band position in the channel to obtain the velocity gradient curve. The integrations to obtain the velocity profile curves and the flow rates were similar to those previously described. Although this method of calculation gave flow rates closer to those actually measured than did the first method, the calculated flow rates were still far smaller than

those actually measured.

A third method of calculation was applied to the data obtained without the use of the quarter-wave plates. The center band was assigned a zero rate of shear and the bands adjacent to the center a rate of shear according to the number of bands of higher shearing stress that had merged with them. Thus, if there had been one merger with each of the first order bands adjacent to the center band, the bands would be assigned a rate of shear corresponding to a second order band. If there had been two mergers with these first order bands, they would be assigned a rate of shear corresponding to a third order band, etc. Integrations by this method gave better results than the two methods previously described. However, the calculated flow rates were lower than the actual flow rates by as much as 52 per cent.

Out of curiosity, a fourth method of calculation was tried using the data obtained with the use of quarter-wave plates. In this method, which was contrary to many principles already stated, the center band was assigned a definite rate of shear corresponding to the number of band mergers. Integration of the velocity gradient curves obtained gave sharp-nosed velocity profile curves. Flow rates calculated from the areas under these profile curves, like the flow rates calculated by other methods, were highly erroneous. Such calculations, even though they involved unsound principles,

were made in order that no methods would be left untried before failure could be established.

A new type of channel was built to study the effect of altering the shearing stress in the line of sight. As described in Chapter IV (page 16), this tube consisted of a square Plexiglas channel in one end of which were fastened parallel to each other four thin metal strips. This type of channel was designed to eliminate the wall effects in the line of sight. In Figure 8 are shown the types of flow patterns that should be produced in both the square channel and the square channel with the metal strips in one end. As in

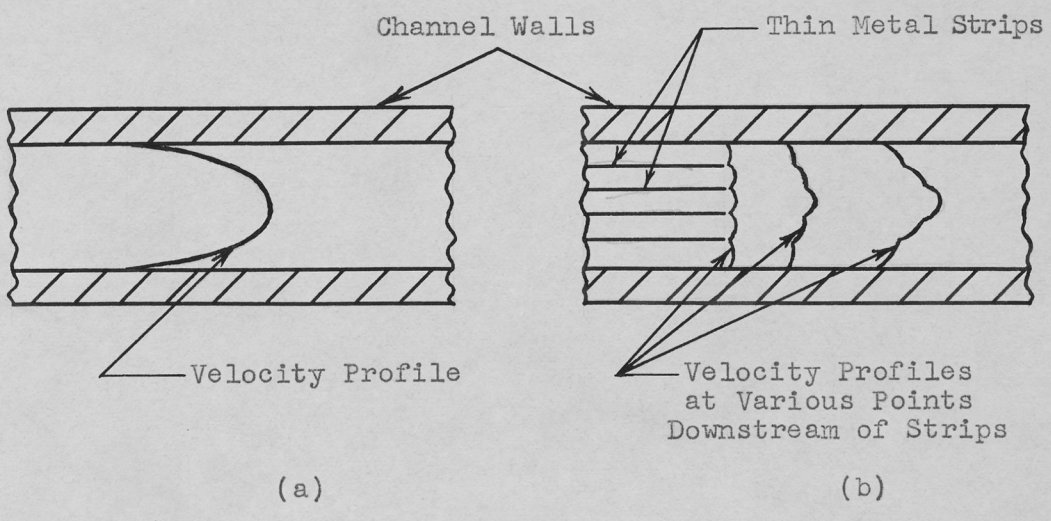


Figure 8. Top views of velocity profiles in square channels. (a) Velocity profile in ordinary square channel. (b) Velocity profiles just downstream of thin metal strips fastened in a square channel.

Figure 8 (b), the effect of the metal strips should be to produce a flatter velocity profile immediately downstream from the end of the strips. However, in actual practice the analysis of the flat velocity profile was impossible. Under flow conditions, a turbulence was produced at the end of the metal strips that distorted the bands beyond any visual analysis. Of course, if observations were made beyond the distorted region, the velocity distribution across the channel would have returned to normal.

Theoretical analysis was made of the flow in a third type of channel. This channel had a horizontal width approximately three times the vertical width. The ratio of horizontal width to vertical width is spoken of as the aspect ratio. In this channel, the effects of the vertical walls on the optical pattern is reduced because the polarized light is passed through a greater thickness of liquid. Analysis of the data taken with this channel proved to be much more satisfactory than the other calculations. The good results are in agreement with expectations, since the larger aspect ratio provides a closer approximation to a two-dimensional flow system.

CHAPTER VII

RESULTS AND DISCUSSION

In Table I on the following page are shown the results of all the calculated flow rates. A presentation is made of the per cent error of the calculated flow rates from the flow rates measured by the rotameter. The method of integration used in each determination is also briefly stated. Reference should be made to Chapter VI for detailed explanation of the various methods of integration used.

The first method of analysis where the merger of bands was disregarded is evidently the most erroneous. When this method of analysis was applied to the data, it was not known that the bands actually did merge with one another. The errors in the flow rates calculated by this method ranged from 63 per cent low for a flow rate of 9 cc. per second to 92 per cent low for a flow rate of 165 cc. per second.

The second method of analysis, using an empirical method of adjusting the band orders, also gave unsatisfactory results. This method used a linear relationship to correct the center band order down to zero with the intermediate bands being corrected a proportional amount down to a zero correction at the walls. The results of these calculations ranged from 30 per cent low for a flow rate of 35 cc. per second to 58 per cent low for a flow rate of 107 cc. per

TABLE I

SUMMARY OF FLOW RATE DETERMINATIONS

Rotameter Setting	Type of Channel	Solution	Per Cent Error in Flow Rate	Method of Integration
40	sq.	T-2	63 - low	Merger of bands disregarded
170	"	"	86 - low	"
170	"	"	90 - low	"
230	"	"	92 - low	"
80	"	"	13 - high	Center band displaced from zero
170	"	"	16 - low	"
80	"	"	30 - low	Data adjusted
170	"	"	58 - low	"
40	"	"	16 - low	Quarter-wave plates out
170	"	"	50 - low	"
80	Sq. with metal strips	T-3	17 - low	"
80	"	"	35 - low	Data adjusted
170	"	"	18 - low	Data adjusted. Disturbed flow pattern.
40	rect.	"	0	Quarter-wave plates in. No adjustment of data needed.
40	"	"	5.5 - high	Quarter-wave plates out

second.

A third method of calculation was applied to the data which were taken without the use of quarter-wave plates. As explained in Chapter VI, a different flow pattern was observed when plane polarized light was passed through the solution from that observed when circularly polarized light was used. These observations differ from the theories presented in Frocht (1). Also it was observed that the orientation of the polarizer and analyzer plates caused changes in the pattern of bands. This was contrary to expectations. In the third method of analysis, the center band was assigned a zero order, the second band an order equal to the number of mergers plus one, etc. Calculations using this method of analysis were a little more encouraging but still in serious error. Calculated flow rates ranged from 16 per cent low for a flow rate of 9 cc. per second to 50 per cent low for a flow rate of 107 cc. per second.

The second and third methods of analysis were applied to data taken from the square channel with the metal strips in one end. Due to the distortion near the end of the metal strips, readings were taken downstream from the strips. At the point where readings were taken, the velocity distribution in the channel had probably resumed its normal shape like the velocity distribution in the ordinary square channel. As would be expected, the results obtained with this

modified square channel were about the same as those obtained with the ordinary square channel. However, one measurement was taken close to the distorted flow region, and calculations were made by the empirical adjustment of the data previously described. The calculated flow rate was only 18 per cent below the actual flow rate of 107 cc. per second. This error is relatively small when compared with an error of 58 per cent for data taken in the square channel at the same flow rate and calculated by the same method,

The fourth method of analysis in which the center band was displaced from zero is invalid because of certain theoretical considerations as well as because of the results it gave. This method involved assigning a non-zero rate of shear to the center band according to the number of band mergers observed under circularly polarized light. Sharp-nosed velocity profiles were the result of the calculations. Work of previous experimenters indicates that such velocity profiles are highly unlikely. The results of this method were 13 per cent high for a flow rate of 35 cc. per second and 16 per cent low for a flow rate of 107 cc. per second.

Enlightening results were obtained by the use of a rectangular channel. This channel had a large aspect ratio, i.e., its horizontal width was three times its vertical width. Only two calculations were made with data from this channel. The results were $\pm$ 1 per cent in error for a flow

rate of 9 cc. per second using quarter-wave plates and 5.5 per cent high for the same flow rate using data taken without the use of quarter-wave plates.

The results in Table I, page 33, indicate that all methods of analysis attempted for square channels gave flow rates lower than those actually measured. The errors are great enough to disprove all the methods of analysis that were tried. It is also easily seen that the errors increase as flow rates increase.

From the results obtained using the rectangular channel, it appears that this method of analysis may be correctly applied to two dimensional flow systems. Two dimensional flow systems are approximated by channels with high aspect ratios, the aspect ratio being defined as the ratio of the width of channel through which polarized light is passed to the other dimension. In passing polarized light through a great thickness of liquid, as in the high aspect ratio channel, the wall effects in the line of sight are greatly reduced. For rectangular channels with aspect ratios of five or even ten, the effects of the side walls in the line of sight may be nearly eliminated. This wider aspect ratio will produce a much flatter velocity profile across the wider tube dimension.

It is believed that in three dimensional flow systems such as those studied in the square channels, a rotation of

the optic axis occurs which affects the optical pattern of bands. This phenomenon is described in more detail by Frocht (2). The rotation of the optic axis is believed to be caused by the shearing stress of the channel walls in the line of sight and will be greatly reduced in channels with high aspect ratios.

CHAPTER VIII

CONCLUSIONS AND RECOMMENDATIONS

The study of flow phenomena using aqueous milling yellow dye solutions is far from complete. Although this work was not extensive enough to prove any definite theories, some enlightening results were obtained.

Conclusions:

1. No method is available at present for determining flow rates through square channels by analyzing the flow patterns produced by a doubly refracting liquid.
2. The results of the previously tried methods of analysis for flow through square channels are all lower than the measured flow rates. The percentage error was also found to increase with increasing flow rates.

Recommendations:

It is recommended that more flow rate analyses be undertaken using rectangular channels of high aspect ratios.

LIST OF REFERENCES

LIST OF REFERENCES

1. Frocht, M. M., Photoelasticity, Volume I, New York: John Wiley and Sons, Inc., 121-125, 136 (1941).

2. Frocht, M. M., Photoelasticity, Volume II, New York: John Wiley and Sons, Inc., 334-338 (1948).

3. Peebles, F. N., Prados, J. W., and Honeycutt, E. H., Jr., "A Study of Laminar Flow Phenomena Utilizing a Doubly Refracting Liquid," Progress Report 1 under Contract Number Nonr-811(04), Knoxville, Tennessee, Engineering Experiment Station and Department of Chemical Engineering of the University of Tennessee (1954).

4. Prados, J. W., Personal Communication (1956).

5. Prados, J. W., "Determination of the Flow Double Refraction Properties of Aqueous Milling Yellow Dye Solutions," Master's Thesis, University of Tennessee (1954).

APPROVAL

The foregoing thesis is hereby approved as a creditable study of an engineering subject, carried out and presented in a manner sufficiently satisfactory to warrant its acceptance as a prerequisite to the degree for which it has been submitted. It is understood that by this approval the undersigned does not necessarily endorse or approve any statement made, opinion expressed, or conclusions drawn therein, but approves the thesis only for the purpose for which it is submitted.

Name John W. Prados

Title Instructor

Date August 17, 1956

APPENDIX

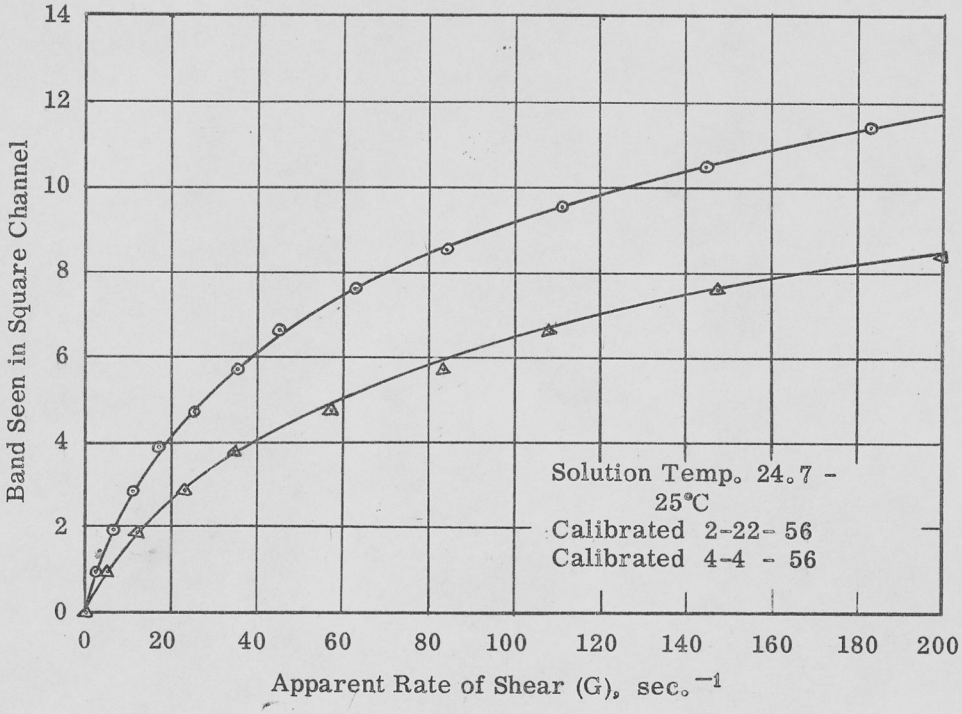


Figure 9. Calibration Curves of Solution T-2.

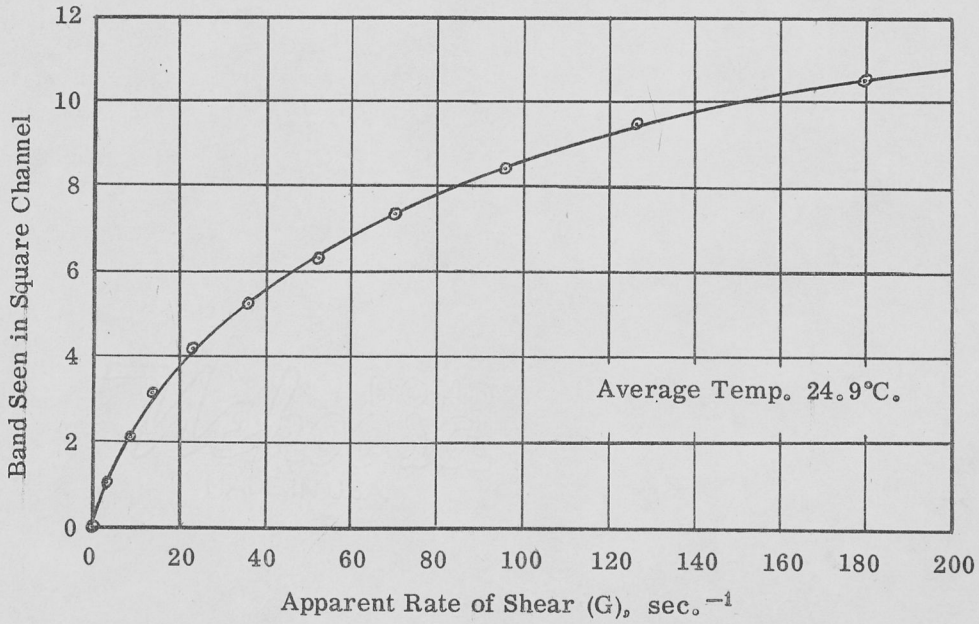


Figure 10. Calibration Curve of Solution T-3.

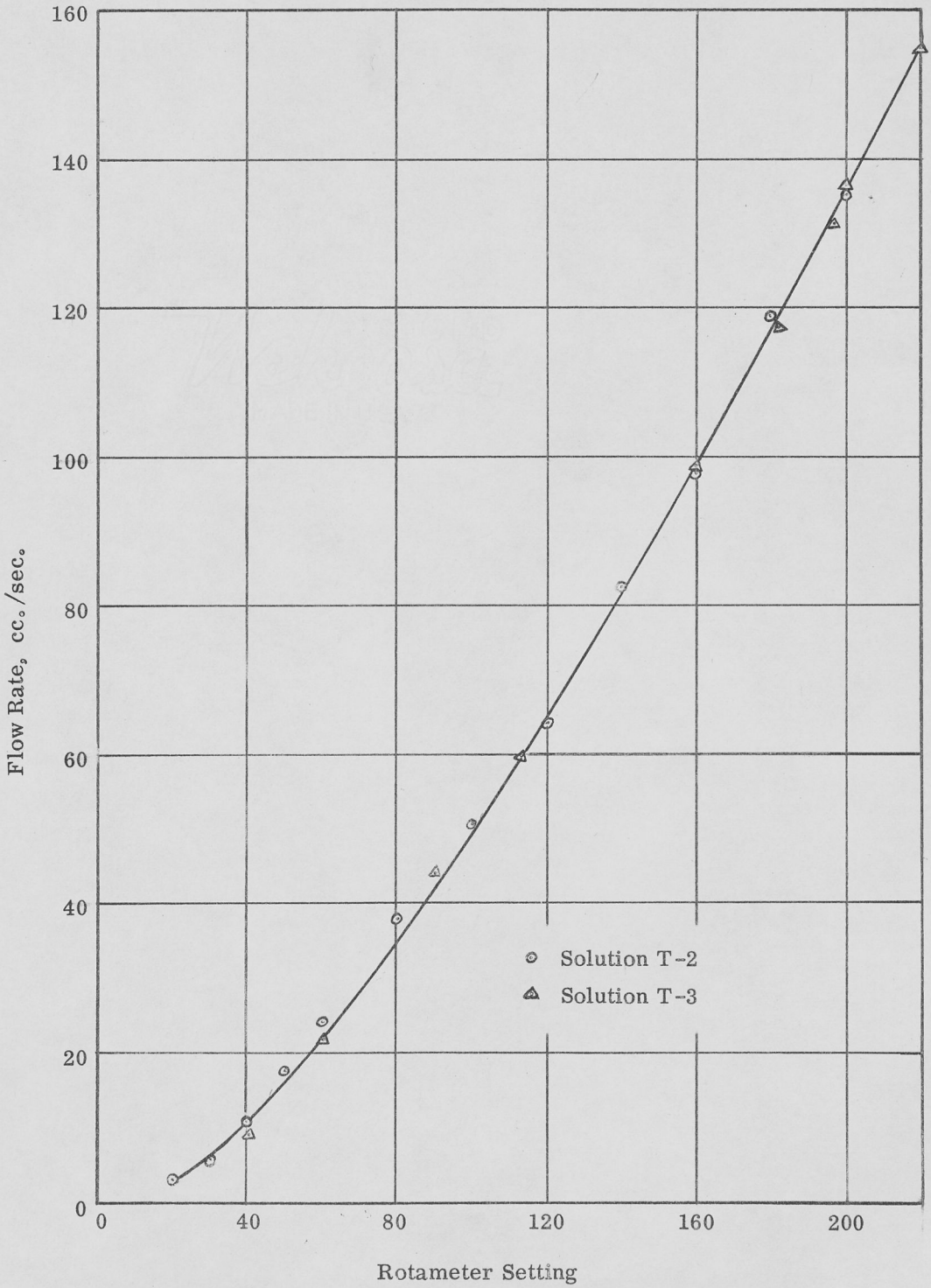


Figure 11. Rotameter Calibration Curve.

TABLE II

CALCULATION OF DATA FOR PLOTTING THE VELOCITY GRADIENT CURVE IN A RECTANGULAR CHANNEL

General Data

Rotameter: 40 ± 1
Date: June 15, 1956 Temperature: 25.0-25.1°C.
Dye Solution: T-3 *Page No.: 14368 (top)

Note: Data taken without quarter-wave plates. No merger of bands observed.

1 Band Number	2 Distance from Top - y (cm.)	3 G(sec.$^{-1}$) Uncorrected	4 G(sec.$^{-1}$) Corrected
top	0.000	-	-
5	.097	32.5	10.3
4	.184	21.5	6.8
3	.288	13.3	4.2
2	.414	7.0	2.2
1	.528	2.5	0.8
0	.650	0.0	0.0
1	.765	2.5	0.8
2	.898	7.0	2.2
3	1.040	13.3	4.2
4	1.130	21.5	6.8
5	1.257	32.5	10.3
bottom	1.324	-	-

*Page numbers refer to University of Tennessee Department of Chemical Engineering Original Record of Research.

EXPLANATION OF TABLE II

Column

1. Band number as observed in rectangular channel.
2. Distance of each respective band as measured from the top of the channel in centimeters.
3. The rate of shearing stress (G) measured in seconds^{-1} corresponding to each respective band. These data were obtained from Figure 10, page 42.
4. The corrected rate of shearing stress. The calibration curve shown in Figure 10 was calculated for a channel 1.2 cm. in width. The rectangular channel in this determination was 3.80 cm. in width. Column 3 was multiplied by the ratio of 1.20:3.80 to correct for the added liquid depth.

Figure 12 is a plot of column 4 versus column 2, Table II.

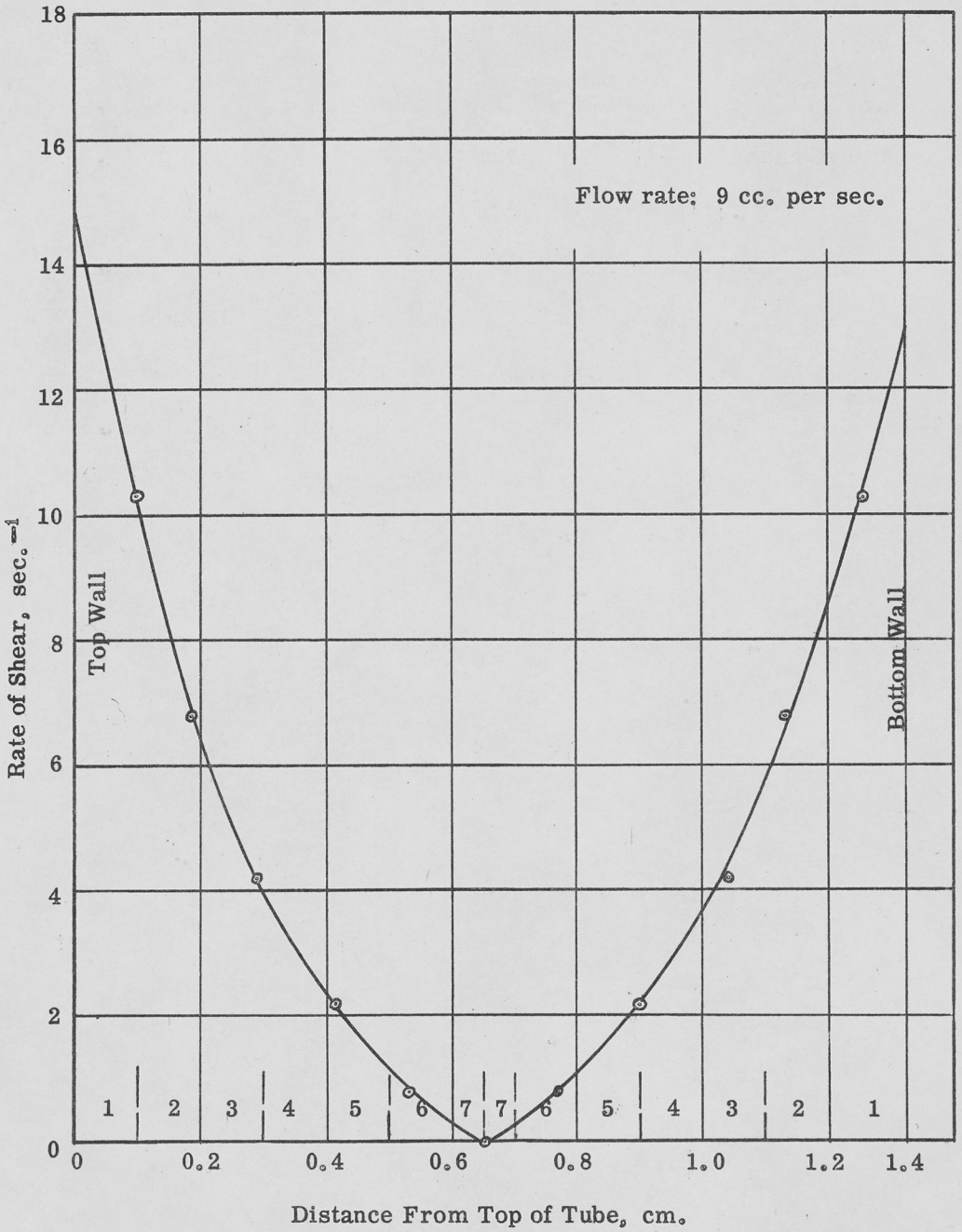


Figure 12. Velocity Gradient Across Rectangular Channel.

TABLE III

CALCULATION OF DATA FOR PLOTTING THE VELOCITY PROFILE CURVE IN A RECTANGULAR CHANNEL

1	2	3	4	5
Area No. from Left	$\overline{G}$ (sec.$^{-1}$)	$\overline{G}\Delta y$ (cm.-sec.$^{-1}$)	y (cm.)	Velocity (v) (cm./sec.)
1	12.6	1.26	0.1	1.26
2	8.2	0.82	.2	2.08
3	5.2	.52	.3	2.60
4	3.2	.32	.4	2.92
5	1.8	.18	.5	3.10
6	0.6	.06	.6	3.16
7	.1	.01	.65	3.17
Area No. from Right				
1	10.6	1.06	1.2	1.06
2	7.0	0.70	1.1	1.76
3	4.5	.45	1.0	2.21
4	2.9	.29	0.9	2.50
5	1.6	.16	.8	2.66
6	0.6	.06	.7	2.72
7	.1	.01	.65	2.73

EXPLANATION OF TABLE III

Column

1. Area number of Figure 12, page 47, as measured from left to center and then from right to center. Area No. 1 from the left includes the area under the curve in Figure 12 between a y of 0.0 and 0.10. Area No. 2 from the left includes the area under the curve between a y of 0.10 and 0.20, etc.
2. The average rate of shearing stress (G) under each respective interval in seconds^{-1}.
3. The area under each interval of the curve numbered in Column 1. This area is obtained by multiplying the average shearing stress ($\overline{G}$) by the interval distance at the base of the curve (Δy).
4. The distance (y) in cm. at which the area determined in Column 3 is to be applied.
5. The velocity in cm. per second at the point in the channel given in Column 4. The velocity is obtained by adding together successively the areas given in Column 3.

Figure 13 is a plot of Column 5 versus Column 4. This curve gives the average velocity distribution across the channel. An average curve has been drawn between the velocities given by the area to the left of the center and the area to

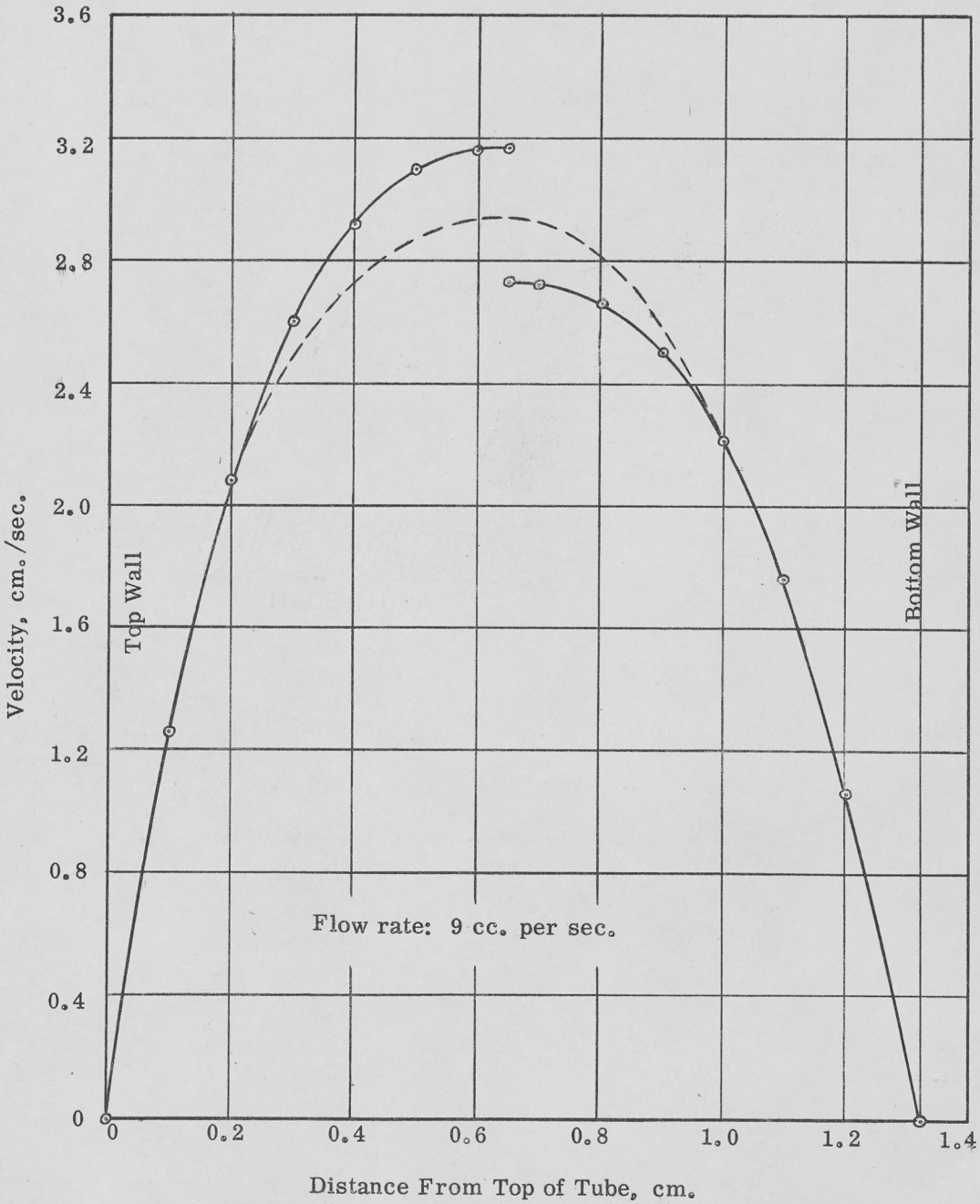


Figure 13. Velocity Profile Across Rectangular Channel.

the right of the center.

Evaluation of the Area Under the Velocity Curve (Figure 13) by Simpson's Rule:

$$A = 1/3\ h\left[(y_o + y_n) + 4(y_1 + y_3 + y_5 + \ldots) + 2(y_2 + y_4 + y_6 + \ldots)\right]$$ Simpson's Rule

where

A = area under the curve

h = width of the even number of intervals into which the curve is divided = 0.1 cm.

y_n = velocity at end of each interval as determined from the curve in Figure 13.

$$A = 1/3(0.1)\left[(0 + 2.16) + 4(1.25 + 2.55 + 2.90 + 2.93 + 2.67 + 1.85) + 2(2.08 + 2.78 + 2.95 + 2.85 + 2.39)\right]$$

$$A = 1/3(0.1)\left[2.16 + 4(14.15) + 2(13.05)\right]$$

$A = 2.83$ sq. cm./sec.

Area of interval number 13:

$$A = \bar{v}\Delta y = (0.55 \text{ cm./sec.})(0.12 \text{ cm.})$$
$$= 0.07 \text{ sq. cm./sec.}$$

Total Area = 2.83 + 0.07 = 2.90 sq. cm./sec.

Volumetric flow rate through rectangular channel = area under velocity curve x width of channel:

$$Q = (2.90 \text{ sq. cm./sec})(3.80 \text{ cm.}) = \underline{11.0 \text{ cu.cm./sec.}}$$

Rotameter calibration of solution T-3 gives:

$$Q = 10.9 \text{ cu. cm./ sec.}$$

$$\text{Per cent error} = \frac{11.0 - 10.9}{10.9} (100) = 0.9$$

CRANES CREST

TABLE IV

CALCULATION OF DATA FOR PLOTTING THE VELOCITY GRADIENT CURVE IN A SQUARE CHANNEL

General Data

Date: April 15, 1956
Rotameter: 170 ± 1
Dye Solution: T-3
Temperature: 24.7-25.0°C
Page No.: 14364

Note: Data taken without quarter-wave plates. Bands merged as indicated in the first column.

Band Number	Distance from Top - y (cm.)	Shearing Stress (G) ($sec.^{-1}$)
top	0	-
8	0.084	172
7	.156	122
6	.230	87
5	.321	61
4	.422	41
0	.606	0
4	.779	41
5	.912	61
6	1.032	87
7	1.108	122
8	1.172	172
bottom	1.205	-

Note: All columns in the table have the same significance as those in Table II, page 44.

Figure 14 is plotted from the last two columns in the above table.

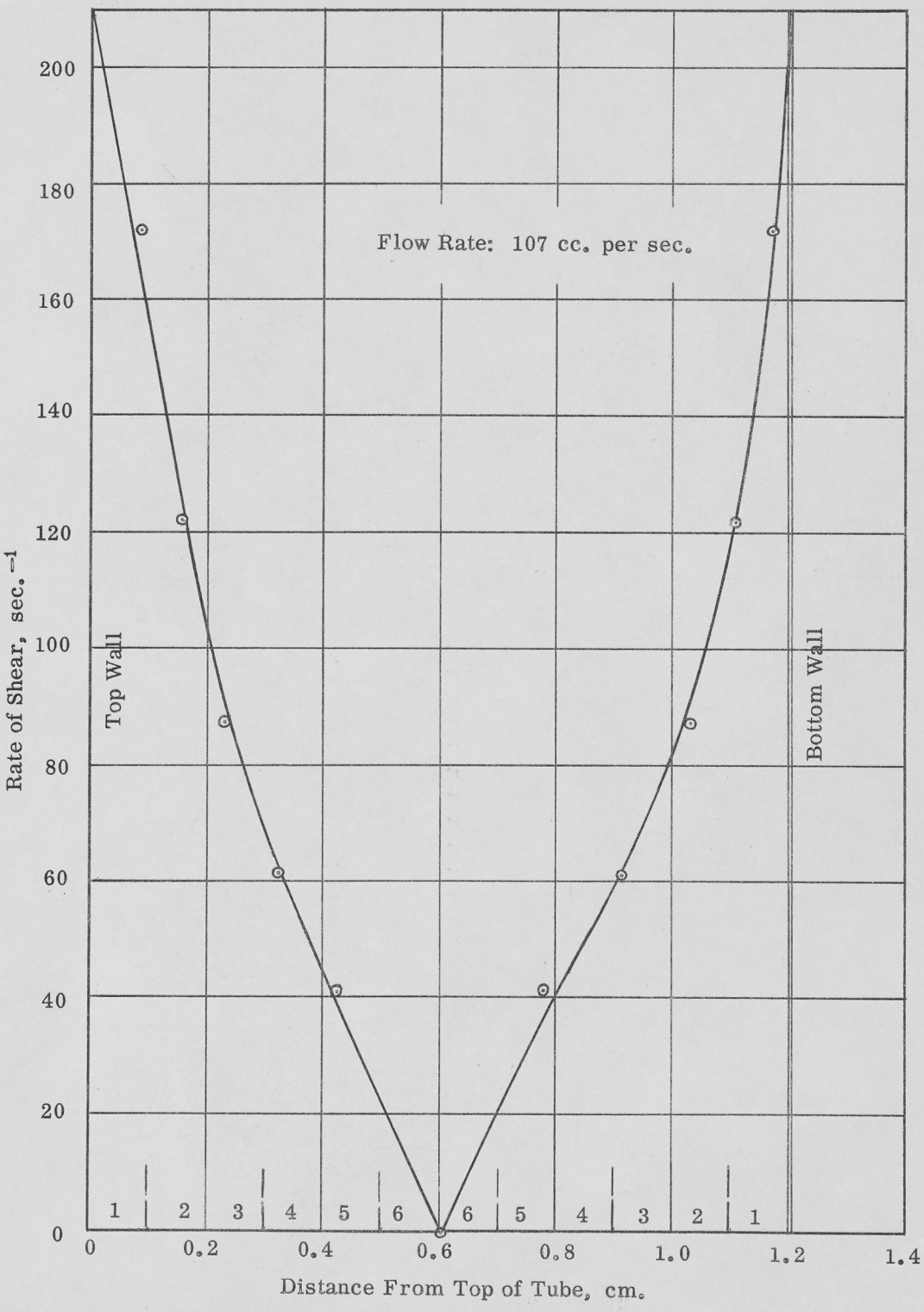


Figure 14. Velocity Gradient Across Square Channel.

TABLE V

CALCULATION OF DATA FOR PLOTTING THE VELOCITY PROFILE CURVE IN A SQUARE CHANNEL

Area No. from Left	$\bar{G}$ (sec.$^{-1}$)	$\bar{G}$ y (cm.-sec.$^{-1}$)	y (cm.)	Velocity (v) (cm./sec.)
1	185	18.5	0.1	18.5
2	128	12.8	.2	31.3
3	80	8.0	.3	39.3
4	56	5.6	.4	44.9
5	34	3.4	.5	48.3
6	12	1.3	.606	49.6
Area No. from Right				
1	156	16.4	1.1	16.4
2	96	9.6	1.0	26.0
3	68	6.8	0.9	32.8
4	53	5.3	.8	38.1
5	36	3.6	.7	41.7
6	13	1.3	.606	43.0

Note: All columns in the table have the same significance as those columns in Table III, page 47.

Figure 15 is plotted from the last two columns in the above table.

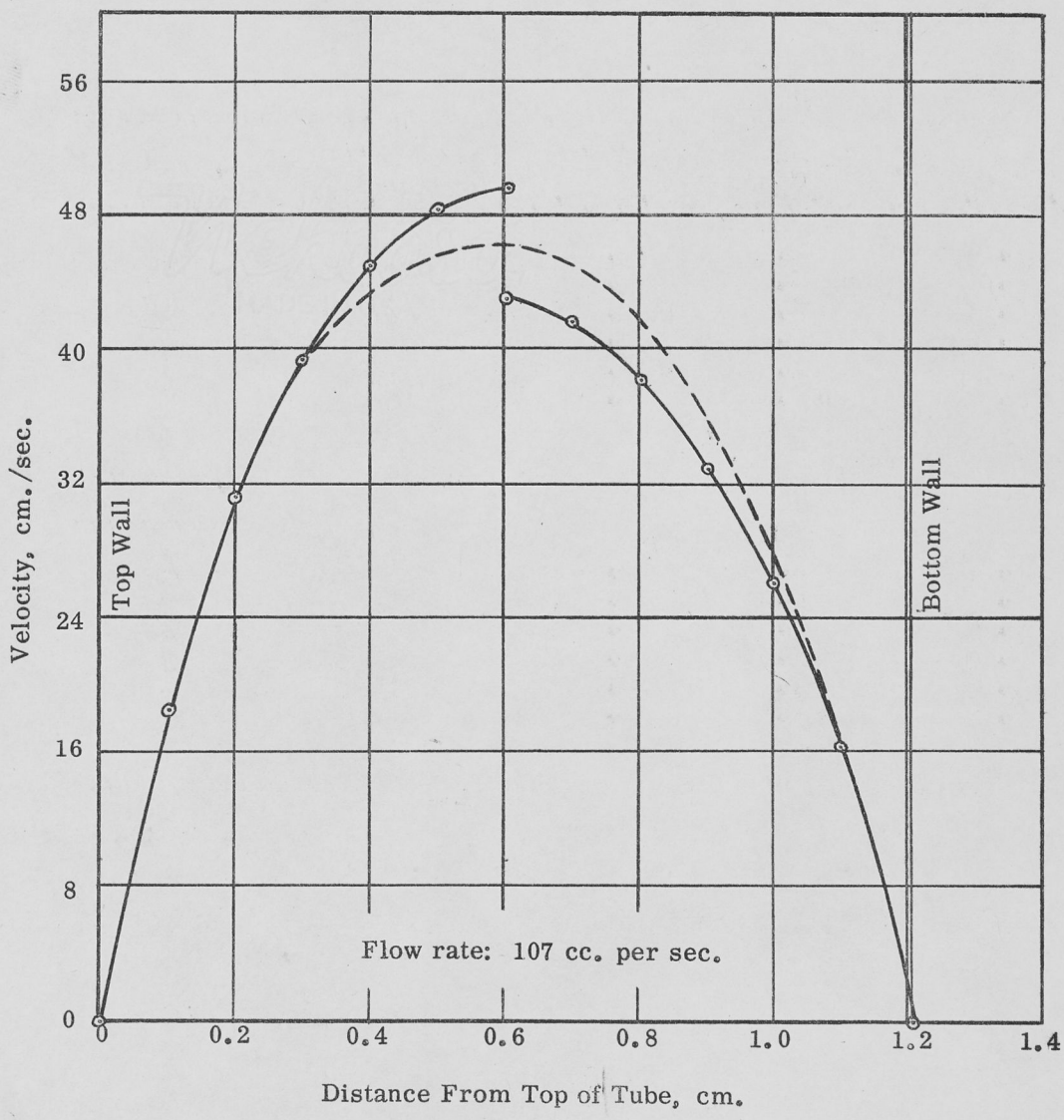


Figure 15. Velocity Profile Across Square Channel.

Evaluation of the Area Under the Velocity Curve (Figure 15) by Simpson's Rule:

$A = 39.4$ sq. cm./sec.

Volumetric flow rate through square channel = area under velocity curve x width of channel:

$Q = (39.4 \text{ sq. cm./sec.})(1.36 \text{ cm.}) = 53.6$ cu. cm./sec.

Rotameter calibration of solution T-3 gives:

$Q = 107$ cu. cm./sec.

Per cent error = 50

CRANE'S CREST

TABLE VI

EXPERIMENTAL DATA

General Data

	Run 1	Run 2	Run 3
Date:	12-24-55	12-27-55	12-27-55
Rotameter:	170 ± 1	170 ± 1	80 ± 1
Quarter-wave plates:	in	in	in
Solution:	T-2	T-2	T-2
Channel:	square	square	square
Temperature (°C.):	24.0-24.5	24.0-24.6	24.0-24.6
*Page:	14351(bottom)	14352(top)	14353(top)

Run 1		Run 2		Run 3	
Band No.	y (cm.)	Band No.	y (cm.)	Band No.	y (cm.)
top	0.000	top	0.000		
6	.112	6	.122	top	0.000
5	.178	5	.171	5	.094
4	.260	4	.237	4	.175
3	.351	3	.336	3	.259
2	.423	2	.424	2	.360
1	.514	1	.512	1	.461
0	.631	0	.625	0	.610
1	.746	1	.710	1	.730
2	.823	2	.805	2	.823
3	.897	3	.886	3	.923
4	.978	4	.952	4	.999
5	1.049	5	1.055	5	1.063
6	1.087	6	1.119	bottom	1.193
bottom	1.202	bottom	1.198		

*Page numbers refer to University of Tennessee Department of Chemical Engineering Original Record of Research.

TABLE VII

EXPERIMENTAL DATA

General Data

	Run 1	Run 2	Run 3
Date:	12-28-55	12-29-55	1-1-56
Rotameter:	40 ± 2	230 ± 1	80 ± 1
Quarter-wave plates:	in	in	in
Solution:	T-2	T-2	T-2
Channel:	square	square	square
Temperature (°C.):	24.7-25.0	23.0-23.2	24.6-24.8
Page:	14356	14357	14358

Run 1		Run 2		Run 3	
Band No.	y (cm.)	Band No.	y (cm.)	Band No.	y (cm.)
		top	0.000		
		8	.076		
		7	.123		
		6	.180	top	0.000
		5	.242	5	.109
top	0.000	4	.314	4	.181
3	.109	3	.370	3	.263
2	.227	2	.426	2	.351
1	.430	1	.524	1	.450
0	.608	0	.584	0	.602
1	.748	1	.677	1	.746
2	.959	2	.766	2	.835
3	1.117	3	.816	3	.936
bottom	1.204	4	.883	4	1.019
		5	.948	5	1.095
		6	1.021	bottom	1.222
		7	1.085		
		8	1.147		
		bottom	1.231		

TABLE VIII

EXPERIMENTAL DATA

General Data

Date: 2-20-56
Channel: square
Solution: T-2

Temperature (°C.): 24.8-25.1
Quarter-wave plates: in
Page: 14361

Bands Converged to Center Band	Rotameter Setting	Average Rotameter Setting at Merger
1	29-32	30.5
2	44-48	46.0
3	54-58	56.0
4	100-106	103.0
5	154-159	156.5
6	225-250	237.5
1	31-38	34.5
2	47-54	50.5
3	66-78	72.0
4	110-131	120.5
5	162-198	180.0
6	250	250.0

TABLE IX

EXPERIMENTAL DATA

General Data

	Run 1	Run 2	Run 3
Date:	4-9-56	4-15-56	5-21-56
Rotameter:	40 ± 1	170 ± 1	80 ± 1
Quarter-wave plates:	out	out	out
Solution:	T-2	T-2	T-3
Channel:	square	square	sq. with strips
Temperature (°C):	24.8-25.0	24.7-25.0	25.0-25.1
Page:	14362	14364	14365(top)

Run 1		Run 2		Run 3	
Band No.	y (cm.)	Band No.	y (cm.)	Band No.	y (cm.)
				top	0.000
		top	0.000	6	.055
		5	.084	5	.130
top	0.000	4	.156	4	.192
3	.058	3	.230	3	.278
2	.205	2	.321	2	.372
1	.361	1	.422	1	.472
0	.577	0	.606	0	.671
1	.805	1	.779	1	.891
2	.980	2	.912	2	.986
3	1.131	3	1.032	3	1.075
bottom	1.185	4	1.108	4	1.157
		5	1.172	5	1.236
		bottom	1.205	6	1.289
				bottom	1.336

TABLE X

EXPERIMENTAL DATA

General Data

	Run 1	Run 2	Run 3
Date:	5-21-56	5-21-56	6-12-56
Rotameter:	80 ± 1	170 ± 1	40 ± 1
Quarter-wave plates:	in	in	in
Solution:	T-3	T-3	T-3
Channel:	sq. with strips	sq. with strips	rectangular
Temperature (°C):	approx. 25.0	24.5-24.7	24.5-25.5
Page:	14365 (bottom)	14366	14367

Run 1		Run 2		Run 3	
Band No.	y (cm.)	Band No.	y (cm.)	Band No.	y (cm.)
		top	0.000		
		9	.060		
		8	.111		
top	0.000	7	.286		
6	.090	6	.357	top	0.000
5	.185	5	.393	5	.083
4	.243	4	.426	4	.198
3	.300	3	.458	3	.310
2	.383	2	.527	2	.423
1	.498	1	.601	1	.533
0	.651	0	.629	0	.655
1	.809	1	.657	1	.773
2	.902	2	.726	2	.924
3	.996	3	.783	3	1.052
4	1.093	4	.824	4	1.182
5	1.168	5	.890	5	1.205
6	1.242	6	.963	bottom	1.288
bottom	1.340	7	1.068		
		8	1.160		
		9	1.241		
		bottom	1.277		

TABLE XI

EXPERIMENTAL DATA

General Data

	Run 1	Run 2
Date:	6-16-56	6-16-56
Quarter-wave plates:	in	out
Solution:	T-3	T-3
Channel:	sq. with strips	sq. with strips
Page:	14369 (top)	14369 (bottom)

Run 1		Run 2	
Bands Merged with Center Band	Rotameter Setting	Bands Merged with Bands Adjacent to Center Band	Rotameter Setting
0	0-56	0	0-50
1	56-61	1	50
2	95	2	80
3	165	3	120
		4	240